MULTIDISCIPLINARY OPTIMIZATION OF AN AIRCRAFT WING/TIP STORE IN THE TRANSONIC REGIME

BY

SRINIVASAN JANARDHAN, RAMANA V. GRANDHI
Dept. of Mechanical & Materials Engg.
Wright State University
Dayton, OH 45435

Submitted to

JOURNAL OF ENGINEERING OPTIMIZATION
United Kingdom
July 2003

Multidisciplinary Optimization of an Aircraft Wing/Tip Store Configuration in the Transonic Regime

Srinivasan Janardhan[*] *and Ramana V. Grandhi*[†]

Wright State University

Dayton, Ohio 45435, U.S.A.

Abstract: In this research, a multidisciplinary optimization procedure is described to delay the occurrence of store-induced flutter of an aircraft wing/tip store configuration. A preliminary design procedure was developed to enhance the performance characteristics of an aircraft wing model in the transonic Mach number regime. A wing/tip store configuration with the store center of gravity (c.g.) located at the 50% aerodynamic tip chord was chosen for structural optimization. The aircraft wing structural weight was chosen as the objective function with constraints on natural frequency, stress and flutter. Automated Structural Optimization System (ASTROS) and Computational Aeroelasticity Program-Transonic Small-Disturbance (CAP-TSD) were the computational tools employed to perform the structural optimization and subsequent aeroelastic (mutual interaction between the aerodynamics and structural deformation) analysis in the transonic regime. This work showed that an improved store-induced flutter speed was obtained by increasing the separation between the first two

[*] Graduate Research Assistant, Department of Mechanical and Materials Engineering, Wright State University, Dayton, Ohio 45435, U.S.A., Email: sjanard@cs.wright.edu

[†] Distinguished Professor, Department of Mechanical and Materials Engineering, Wright State University, Dayton, Ohio 45435, U.S.A., Email: rgrandhi@cs.wright.edu

natural frequencies of the wing structure. These results were compared with the results of those cases in which the flutter constraints were incorporated, along with the stress and frequency constraints, in the optimization problem. The addition of the flutter constraint resulted in a negligible increase in flutter speed when compared with the flutter speed obtained from optimization with only frequency and stress constraints.

Keywords: store-induced flutter, CAP-TSD, ASTROS, aeroelasticity, transonic, optimization.

Introduction

The attachment of external stores to a clean wing causes several dynamic aeroelastic instabilities. These instabilities could be in the form of flutter or limit-cycle oscillations (LCO). Such phenomena are a major hindrance to the efficient operation of a fighter aircraft carrying out mission-critical tasks. This hindrance has more impact when the aircraft is passing through the transonic regime. The nonlinear and dual characteristics (subsonic and supersonic) of the transonic regime make it complex and difficult to analyze. The sustained effect of store-induced instabilities (flutter) can lead to catastrophic consequences. The presence of stores, especially tip stores, can lead to several problems in the target-locking of an air-to-air missile attached at the wing tip and the roll maneuverability of the entire aircraft. The occurrence of such unstable vibrations must be considered seriously and eliminated during the preliminary design of wing structures. A military flight vehicle free of store-induced dynamic aeroelastic phenomena during its entire mission-related operational envelope is the requirement of an aircraft structural designer. Usually, the optimization or adjustment of the stiffness, mass distribution or aerodynamic parameters of a clean wing results in a flutter-free design. However, the attachment of external stores to a fighter aircraft wing results in flutter instability occurring at reduced flight speeds. To avoid such an early occurrence of flutter instability, design constraints are placed on the operation of the flight vehicle so as to enhance the flutter onset speed to a higher flight speed.

In the past, the majority of research efforts were focused mainly to predict the occurrence and computation of dynamic aeroelastic stability boundaries (flutter). Very few researchers developed computationally robust methods to perform the optimization of an

aircraft wing in the transonic regime. This is because of the fact that aircraft structural design is often accomplished through a series of design iterations. These iterations are computationally intensive and require large computational time. Moreover, this iterative process does not guarantee a design of minimum weight for all the design conditions since the designer's judgment and intuition are influencing factors in the redesign process and only a small number of design iterations are practical. Even with the aid of the digital computer, the design of complex structures to satisfy dynamic response restrictions has been hampered by the inherent difficulty and the computational cost of dynamic analysis. Recent advances in programming techniques and matrix methods of structural analysis have provided all the necessary tools for the development of efficient aircraft structural optimization methods. In principle, there are many ways in which an optimum design of a structure may be found; essentially, the problem is that of developing an efficient design procedure that utilizes a reasonable amount of computer storage and execution time to find the optimum design of a complex structure.

The purpose of this research is to implement an optimization technique for developing a minimum weight design of an aircraft wing structure connected to a tip store when subjected to frequency, stress and flutter constraints. In the process of developing an optimum wing design, the main objective is to delay the occurrence of dynamic aeroelastic phenomena such as store-induced flutter. This delay in the occurrence of flutter was intended over a Mach number range of M 0.8-0.96 in the transonic regime, which most of the fighter aircraft pass through, while moving from the subsonic to supersonic regime. The transonic regime is a nonlinear region, where optimization involves a large number of iterations to arrive at an optimum design. This is due to the presence of nonlinear aerodynamic shocks acting in the

transonic region. So an attempt was made to demonstrate if a reasonably accurate optimized flutter solution could be obtained, based on the linear aerodynamics, in order to save computational cost and time. The computational tool used for performing structural optimization was Automated STRuctural Optimization System (ASTROS)[1]. The nonlinear aeroelastic analysis is performed using Computational Aeroelasticity Program-Transonic Small-Disturbance (CAP-TSD)[2], which has proved in the past to be accurate when performing unsteady aeroelastic analysis in the nonlinear region. The vibration modes obtained from the ASTROS modal analysis were used by CAP-TSD during the aeroelastic analysis to model the structure. Flutter analysis of the optimized wing structure was carried out in both subsonic and transonic regimes using CAP-TSD and then compared with the corresponding ASTROS flutter results to demonstrate if nonlinear aerodynamic analysis is needed during optimization. The increase in flutter speed will help in increasing the flight envelope and accomplishing the mission-critical tasks. This research facilitates in the development of a simulation-based flutter-free wing design for a given range of Mach numbers in the transonic region. Currently, verification of the design requirements for flutter in the transonic regime are almost satisfied entirely by either wind tunnel models or actual flight tests. These methods – although effective – are very costly, dangerous, and time-consuming. The development of a flutter-free design will facilitate in obtaining similar information as the experimental tests so as to reduce the number of flight tests to a few critical ones in the future store certification efforts.

Previous Literature

In recent years, there has been increasing interest in the multidisciplinary design optimization of aircraft structures free of dynamic aeroelastic instabilities occurring caused by the interaction between the air flow and the wing structure. This has led to the implementation of several optimization methods capable of developing structural designs that provide a safe flight envelope in various flow regimes. One of the flow regimes of importance is the transonic regime where the occurrence of flutter is critical.

Recently, Jun et al. [3] studied the influence of a tip missile on the design optimization of a wing structure. A multidisciplinary optimization technique was used to compensate/restore the lost aeroelastic performance due to the presence of the store. A built-up wing box structure was optimized with constraints on static strength and flutter speed. The thickness and the cross-sectional areas of the structural elements were the primary variables in the optimization. However, this optimization study was conducted mainly for the subsonic and supersonic region without including any modal-based constraints. In another study, the influence of a tip store on transonic aeroelastic stability has been examined by Guruswamy et al. [4]. He conducted flutter analysis for rectangular and fighter type wings with tip stores using ATRAN3S code in the transonic region. It was shown that the tip store could make the wing aeroelastically unstable. However, no optimization studies were conducted to suppress or prevent the flutter instability. Striz et al. [5] utilized the doublet-lattice and kernel function methods to investigate the validity of a flat-plate store approximation in comparison to store models of other geometries for an F-5 wing with a tip-mounted launcher/store combination. In

that study various store cross-sections were found to show improved results with only a moderate increase in model complexity and, thus, an increase in computing cost.

Raveh et al. [6] conducted a study, integrating computational fluid dynamics (CFD)-based maneuver loads into a structural design optimization scheme that accounted for stresses and static aeroelastic considerations. However, no optimization was conducted with the dynamic aeroelastic constraints for which the tip store is attached. Kim and Lee [7] performed aeroelastic analyses in the transonic and supersonic flow regions using a CFD technique (TSD3KR) for computing the unsteady aerodynamics in conjunction with MSC/NASTRAN for the flutter analysis of a wing with a tip store. They conducted a matched-point flutter analysis to obtain the flutter solutions in both the frequency and time domain. They showed that the effect of tip store could change the flutter stability of the wing structure significantly. Rudisill and Bhatia [8] developed a numerical procedure to determine the wing structural parameter values, such that a specified flutter speed constraint was satisfied and the structural mass was kept to a relative minimum. This procedure was applied to the design of a box beam. The design of the wing structure, however, was implemented without attaching any tip store. Khot et al. [9] recently conducted a frequency based optimization using smart actuating elements embedded in the composite wing structure to enhance flutter speed. It was found that a higher flutter speed with a minimum structural weight could be obtained when smart actuating materials were used.

Optimization Problem Formulation

The occurrence of store-induced flutter onset speed is increased using constrained optimization methodology. The problem under consideration is as follows – determine the design variables of the wing structure so as to minimize the weight of the wing design such

that the multidisciplinary performance constraints are satisfied. In this constrained optimization problem, the objective function and the associated constraints are defined as follows:

Minimize

$$w(x) = w(x_1, x_2, x_3 \ldots\ldots x_n)$$

where $x_1, x_2, x_3, \ldots\ldots x_n$ are the design variables

subjected to inequality constraints

$$g(X) = g_i(x_1, x_2, x_3 \ldots\ldots x_n) \leq g_i \quad i = 1,2,\ldots\ldots k$$

and the lower and upper bounds on the design variables, also known as the side constraints,

$$x_i^L \leq x_i \leq x_i^U$$

where x_i^L and x_i^U are the lower and upper bounds on each of the design variables.

In the initial phase of the optimization, the wing structure model described in Ref. 10 was implemented. The physical design variables were the thickness of the skins, spars, and ribs of the initial wing structure. The thicknesses of the posts connecting the top and bottom skins were not considered as design variables as they were found to be insensitive to structural optimization. In order to reduce the large computational time in optimization, the number of design variables was reduced using a design variable linking technique for the top and bottom skin variables. As a result, the design variables of all the top skin elements were made equal to their corresponding bottom skin elements.

Usually, in the preliminary design of military aircraft, the objective function is the weight of the wing structure. The weight of the wing consists of the sum of the weights of the elements in the finite element model and of any non-structural attachments. The non-structural

weights are independent of the design variables and, usually, are not included in the objective function. The constraints applied to the design are stresses that are developed under the application of static loads. These static loads are also representative of the applied maneuver loads, which include both aerodynamic and inertia loads at the peak of the maneuver. The total vertical component of the static load applied on the nodes of the wing design was 52,500 pounds. In this study, the stress constraints applied were based on static and dynamic aeroelastic cases. In addition to stress constraints, frequency and flutter constraints were also applied.

The optimization was performed using the multidisciplinary optimization software package ASTROS. This package was chosen due to its ability to integrate aerodynamics and the structures that happen to be the driving force behind the design of aircraft structures represented by the wing, fuselage, etc. ASTROS uses the modified feasible directions algorithm for optimization and the P-K method for computing the flutter speed.

The program tool CAP-TSD was used to perform the aeroelastic analysis of optimized wing designs in the subsonic and transonic regions so as to demonstrate the need for the inclusion of nonlinear (transonic) aerodynamics in the optimization. CAP-TSD utilizes the Transonic Small-Disturbance (TSD) theory to solve unsteady aeroelastic problems in realistic aircraft configurations. The CAP-TSD code uses a time-accurate approximate factorization (AF) algorithm to produce an efficient solution to the unsteady TSD equation. The AF algorithm consists of a time-linearization procedure coupled with an internal subiteration technique. For unsteady flow calculations, the solution is achieved in two steps. First, a time-linearization step is performed to determine an estimate of the potential field. Second, subiterations are performed to minimize the linearization and factorization errors. CAP-TSD

is capable of treating combinations of lifting surfaces and bodies. The advantage of using TSD formulation is the relatively low computational cost compared to other CFD–based models, the simplicity of grid generation and geometry preprocessing, and the ability to treat complete aircraft configuration.

Wing Structure Model

Figure 1 illustrates the finite element model of the wing structure. It is modeled using 120 finite elements – out of which 48 plate bending elements are used to represent the wing top and bottom skins, 42 shear panels to represent the spars and ribs, and 30 rod elements to represent the posts that are used to connect the upper and lower skin nodes. The material used is aluminum ($E=10.3 \times 10^6$ psi).

The wing root is fully constrained at all the structural nodes. No other constraints have been applied at the other nodes and all have six degrees of freedom. The structural weight of the wing is 90.7 lbs. The ratio of non-structural weight to structural weight is 4.16. The non-structural weight, added at various structural nodes, represents the weight of the structure at the outer edges (at the leading and trailing edges) and is attached to the wing and consists of other miscellaneous weights, such as fuel, control systems, etc.

Wing Aerodynamic Model

An aerodynamic model of the wing was developed to provide unsteady aerodynamics for the flutter analysis using doublet-lattice theory as shown in Figure 2. There are 20 spanwise and 20 chordwise panels in the model. The spanwise and chordwise panels are equally spaced. The aerodynamic parameters are calculated at the aerodynamic grids, which,

generally, do not coincide with the structural grid points. A splining technique was used to transfer the structural displacements and aerodynamic forces from one set of grids to the other.

In the case of CAP-TSD, the wing was also modeled in both the physical and computational domain. The physical region boundary of the wing was defined in a manner similar to the ASTROS aerodynamic model. All of the dimensions in the CAP-TSD model were normalized using the reference chord length (in this case, the aerodynamic root chord).

The CAP-TSD computational grid chosen for the wing has 90 streamwise gridlines (with 50 gridlines per wing chord), 30 spanwise gridlines (with 20 gridlines on the wing), and 60 vertical grid lines.

Store Model

The store is attached to the wing at the tip. Figure 3 shows the structural model of the store c.g. connected to the wing at 50% of the aerodynamic tip chord. This configuration was chosen as it represented the worst case scenario in terms of the lowest store-induced flutter speed in the transonic region. The store structural model is represented using six beam elements of equal length. The store is joined to the wing also using beam elements. The attachments are configured in a V-shape. Each end of the connection element is attached to the top skin and bottom skin nodes of the wing tip. It is assumed that the attachments are rigid. The stiffness of material used as attachments is very high compared to the stiffness of store. Figure 4 shows the aerodynamic model of the wing connected to the structural model of the store with its c.g. at 50% tip chord. Only the store inertia property was included in the optimization and analysis as it was found that the store aerodynamics did not affect the store-

induced flutter speed significantly, when compared to the inertia-only store configuration. Therefore, the store aerodynamic model was not developed.

Optimization Results and Discussion

The aircraft wing geometry, i.e., the wing planform, airfoil shape, number of spars and ribs, and spar and rib spacing, was assumed to be fixed. This study was restricted to linear elastic structures. During optimization, the store element thickness values were not considered as the design variables, as the main objective of this research was to design a wing structure based on various performance constraints. The initial wing design selected for the optimization study was the same as in Ref. 10. There were a total of 82 design variables (excluding design variable linking) for all the wing/tip store configurations. The optimization technique was carried out for a range of Mach numbers (M 0.8-0.96) in the transonic region for all the cases. However, the aeroelastic analysis in CAP-TSD was conducted for all the optimized wing designs from the subsonic to the transonic region (M 0.4-0.96). This was done to check the consistency of flutter speed obtained from the optimized results in the subsonic region.

Usually, flutter occurs due to the coupling of the first bending and torsional mode. In order to identify the dominant mode acting and its degree of participation in the occurrence of the flutter phenomenon, four different cases were considered. These cases differed in the constraints applied to the optimization problem:

Case I: Frequency (Mode 1) + Stress constraint applied.

Case II: Frequency (Mode 2) + Stress constraint applied.

Case III: Stress + Frequency (Mode 1 & Mode 2) constraints applied.

Case IV: Stress + Frequency (Mode 1 & Mode 2) + Flutter constraints applied.

In all the above cases, the stress constraints were formulated as Von-Mises stresses for the metallic elements. Von-Mises stresses were applied to the top and bottom skins, ribs, and spars. The design constraint on tensile strength was 64 ksi, on compressive strength, 62 ksi, and on shear strength, 43 ksi. No constraints were applied to the posts that connect the top and bottom skins.

If the modal frequency values of the first two modes are very close to each other, then there is a greater tendency for the flutter to occur. An effort has been made to delay the flutter occurrence by increasing the separation between the first bending mode and torsional mode using structural optimization. The constraint on the first modal frequency, or the bending mode, was applied as atleast a minimum of 4 Hz and the constraint on the second frequency, or torsional mode, was a minimum of 10 Hz. Optimization of the wing design using stress and frequency constraints did not result in any violated constraints during each iteration. This indicates that both the initial and final designs were inside the feasible region.

The behavior of the flutter onset speed of the clean wing and the initial design of the wing/tip store configuration is represented using Figure 5. Flutter behavior is analyzed from the subsonic to the transonic region. The initial design was developed based on real fighter aircraft characteristics. The flutter speed obtained using CAP-TSD, for both the clean wing and the initial wing/tip store configuration design, matched well in the linear subsonic region with their corresponding ASTROS flutter results. This was done to validate the consistency of flutter results at low Mach numbers before venturing into the transonic region. A transonic dip was observed in the nonlinear region for both clean wing and the initial wing/store configuration designs using CAP-TSD. The transonic dip occurs due to the presence of shocks

on the wing surface and shock-induced trailing edge separation, which changes the pressure distribution and, hence, affects the flutter speed. The occurrence of shocks is attributed to the nonlinear interaction between aerodynamic flow and the structure. The aircraft flight envelope decreases due to the occurrence of this transonic dip. The clean wing transonic dip occurs at M = 0.94, while the dip due to the attachment of the tip store occurs at M = 0.92. Thus, there is a shift in the transonic dip due to the attachment of the tip store. This shift in the transonic dip indicates a reduction in the flight envelope of the aircraft. It is this range of flight speed that needs to be broadened by structural optimization so that the aircraft can accomplish its mission-critical tasks more efficiently.

The following flutter speed results comparison shown in Figures 6 and 7 indicates the influence of different constraints have on the optimization. By these comparisons, it will be possible to identify those parameters that affect flutter speed the most during optimization.

Figure 6 shows the comparison of flutter speed between the initial and optimized designs when the Case I (first modal frequency) and Case II (second modal frequency) set of constraints are applied. Optimization of the wing with respect to the first modal frequency resulted in a smaller increase in flutter speed as compared to the second modal frequency. The application of first modal frequency as the constraint resulted in a flutter speed increase of 9.6% at Mach 0.9 using CAP-TSD analysis, while for the second modal constraint, it was 14.26%. Figure 7 represents the comparison of flutter speeds with respect to the Mach number for the initial and optimized wing designs based on Case III and Case IV constraints. The results are shown for the flutter speeds obtained using both ASTROS and CAP-TSD for all the designs. The two optimized designs differed only by the inclusion of the flutter constraint, both had the same stress and frequency constraints. These optimization loops were conducted

over a range of Mach numbers from the subsonic to the transonic regions. There were a total of 66 constraints based on the stress parameter. The combined application of modal frequencies as constraints in Case III showed that even when both modes are applied as constraints, simultaneously, the mode 2 constraint is more dominant than mode 1 and is the one that drives the optimization algorithm. The mode 1 constraint is automatically satisfied. Even though flutter occurs due to mode 1, the driving mechanism behind the delay of store-induced flutter is mode 2. This is due to the fact that the first modal frequency value increases easily from 3.84 Hz to 4.63 Hz due to a small change in the thickness value in some of the elements, causing corresponding minor increase in weight, thereby satisfying one of the constraints. To achieve the required second modal frequency value, the weight of the structure increases further and, along with it, the flutter speed also increases. In spite of the dominant second mode, the flutter mechanism of the resulting optimum design continues to remain the same as the initial design. At Mach 0.92, the flutter speed for the initial design using CAP-TSD analysis is 395.45 knots, while after optimization, the flutter speed increased to 475.12 knots. There is an increase of 16.76% in the flutter speed due to optimization.

CAP-TSD aeroelastic analysis was performed to locate the transonic dip. It was found that the structural optimization pushed the occurrence of the transonic dip to a higher Mach number of 0.94; thereby, increasing the flight envelope of the aircraft in the transonic region. In the case of optimization based on flutter constraint (Case IV), the constraint was applied in such a way that the flutter speed limit was posed as 10-15% more than the flutter speed obtained from the flutter speed using the Case III constraints. The flutter constraint was actually posed on the damping value in ASTROS. However, when the flutter constraint was added, the initial iterations showed some violated constraints, indicating that the initial design

was outside the sample design space. The flutter results show that the inclusion of flutter constraints did not make much of a difference to the optimized design that was obtained using only frequency and stress constraints. The difference in flutter speed between the two optimized designs (Case III and Case IV) was approximately in the range of 1-3% over the Mach number range of interest. Also, addition of the flutter constraint to the optimization problem did not change the flutter mechanism. In both cases, the trend was found to be the same. Even in the nonlinear region, the same mechanism drives the optimization algorithm for both the optimization cases. The transonic dip was found to occur at Mach 0.94 for both cases.

As already known, flutter phenomena in the transonic regime is a nonlinear phenomena. But optimization involving such nonlinear parameters results in excessive computational costs. Therefore, an effort has been made to see if optimization of store-induced flutter phenomena for the transonic regime could be predicted using the linear aerodynamics with reasonable accuracy. Though, there is bound to be some difference between the linear and nonlinear flutter prediction in the transonic region, but if the trend is the same for both the initial and optimized designs over the concerned Mach number, then optimization using nonlinear aerodynamics can be substituted by linear aerodynamics. The option of using linear aerodynamics in optimization reduces the computational cost and time significantly. Figure 8 describes the percentage change in flutter speeds between ASTROS and CAP-TSD for the initial and optimized designs (Cases III and IV). It was observed for the subsonic region that the percent of change for all cases was almost the same. For the transonic regime, there was some difference between ASTROS and CAP-TSD results due to the presence of shocks in the transonic flow process. But this difference remained approximately the same for all the transonic Mach numbers. This suggests that the nonlinear aerodynamics

could be precluded while performing the optimization using CAP-TSD for the transonic region. It was observed that the maximum percentage difference between the ASTROS and CAP-TSD flutter speeds for all the wing designs occurred at M 0.92. The percentage difference for the initial design was 24.31% at Mach 0.92, while the percentage difference was 21.36% for Case III and 21.48% for Case IV. The difference between the percentages for all the Mach numbers was in the range of 1-5%, for both the initial and optimum designs.

In order to gain additional information for making a decision to include nonlinear aerodynamics in the structural optimization, a comparison of the percentage changes between the initial and optimized designs for the ASTROS and CAP-TSD analyses is described in Figure 9. The optimized design cases described here are based on Case III and IV constraints. It was observed that the percentage change was almost the same for all the cases and followed the same trend for the entire Mach number range from the subsonic to the transonic regime. However, the maximum percentage change for all the wing designs was Mach 0.92, while the minimum percentage change was observed at Mach 0.94. The percentage change for the optimized design using Case III was 13.52% for ASTROS and 16.76% for CAP-TSD at Mach 0.92 while, for Case IV, it was 15.69% for ASTROS and 18.73% for CAP-TSD at the same Mach number. The overall change in percentages was lying in the range of 0-4%. This is quite acceptable, given the fact that there is a significant amount of savings in computational time and cost.

Optimization of a wing design usually involves addition and redistribution of material so as to achieve an optimum design. Sometimes, the way the material is distributed can provide an explanation for the occurrence of certain phenomena. Figures 10, 11 and 12 represent the thickness distribution of the upper skin of the initial design and the optimized

designs obtained using Case III and IV constraints. The initial design wing thickness distribution indicates that more material was located at the skin elements connected to the root of the wing along the leading edge. The thickness of the elements gradually decreased from the leading edge towards the trailing edge and from the root chord towards the tip chord. Comparison of the initial and optimized wing designs indicates that the optimizer had increased the thickness of the trailing edge skins and the skins located along the middle spars for the Case III optimized design, while decreasing the thickness of the top skins running along the leading edge spar. Additionally, it can be seen from Table I that these modifications were successful in increasing the gap between the first and second natural frequencies for the optimized designs. The gap was increased from 4.0 Hz to 5.4 Hz, and it resulted in an increase in flutter speed from 450 knots to 524.86 knots at Mach 0.9 for the Case III set of constraints using CAP-TSD. However, there was not much difference in the thickness distribution and flutter velocities between Cases III and IV constraints. It was also observed that more material was distributed along the tip chord close to the trailing edge as compared to the leading edge region along the tip chord. This has resulted in a twist or torsion motion of the wing, which could be one of the reasons for the torsional mode playing a dominant role in the optimization of the wing/tip store design.

Place Table I here

In order to study the effect of optimization on the mode of instability and the severity of flutter, a comparison of the behavior of store-induced flutter mode for the initial and optimized designs using Case III and IV constraints is shown using Velocity-Damping

diagram (V-g) in Figure 13. It was observed that mode 1 is the mode of instability for store-induced flutter in all the wing designs. The optimization did not result in any change of the flutter mechanism. This analysis was conducted using ASTROS at Mach 0.9. It can be seen from Figure 13 that, due to optimization, the slope of the flutter mode and, hence, the severity of occurrence of the flutter has reduced, thereby reducing the wing/tip store's tendency to undergo store-induced flutter. Figure 14 shows the Velocity-frequency (V-ω) diagram comparing the first and second modes of the initial design and the optimized designs. It can be observed that the optimization, using Case III constraints, had resulted in an increase in gap between the first and second modal frequency values, which resulted in an increase in flutter speed and flutter frequency. However, there is not much difference between the results obtained by the addition of flutter constraints (Case IV).

An increase in flutter speed by optimization is usually accompanied by an increase in the structural weight of the wing. But the most important thing to be observed is the amount of increase in flutter speed achieved for a given increase in structural weight. Figure 15 shows the comparison of structural weights of initial and optimized wing designs based on Case III and Case IV constraints. When the stress and frequency constraints (Case III) are applied, the structure is designed for a particular Mach number, and it is used for other Mach numbers as there is no change in the structural dynamics characteristics of the wing with change in Mach number. Therefore, the weight of the optimized wing structure remains constant with respect to Mach number. However, there is a small penalty in weight to increase the flutter speed of the aircraft. It was found that the weight of the structure remained almost the same as Case III when Case IV constraints were applied. At Mach 0.9, the weight of the initial wing design in the wing/tip store configuration with store c.g. at 50% tip chord was 90.7 lbs, while the weight

of the optimized wing design, based on the Case III constraints was 106.23 lbs, and Case IV was 106.22 lbs. Therefore, for a penalty of 15.53 lbs, the flutter speed increases by 74.86 knots using CAP-TSD, for Case III constraints at M 0.9.

Figure 16 shows that all the cases converge at almost the same objective function value in different number of iterations. The final objective function value for wing structural weight was found to be 106.22 lbs for Case IV constraints.

Summary/Conclusions

A multidisciplinary optimization procedure has been implemented to design a wing structure in the transonic region. This effort has been made to enhance the performance characteristics of the wing/tip store configuration by delaying the occurrence of store-induced flutter using structural optimization technique. The increase in store-induced flutter speed was achieved by the separation of the first two natural frequencies. The optimization was performed for four cases, which differed by the constraints that were applied. It was found that the individual application of first bending mode as constraint resulted in a lesser increase in flutter speed, when compared to the second mode. The second mode (torsional mode) was found to be the driving force behind optimization even though store-induced flutter occurred in the first mode. When both the above constraints were applied simultaneously, it resulted in the same increase in flutter speed as the second case. A negligible increase in flutter speed in comparison to the modal frequency constraint was obtained from the flutter constraint approach. The weight increase using both frequency and flutter constraints approaches was approximately the same. It has been found that even though the aerodynamics is nonlinear in the transonic regime, the percentage difference between the ASTROS and CAP-TSD flutter

speed for initial and optimized wing design is approximately the same, both in the subsonic and transonic regions. The ASTROS optimization was able to develop an optimum and feasible wing design with an enhanced flutter speed in the transonic regime. The optimized flutter results were validated using nonlinear aerodynamics. This has increased the flight envelope of the aircraft in the transonic regime, thereby accomplishing the mission-critical tasks. The optimization using the separation of natural frequencies results in less computational time and cost involved than the flutter constraint approach.

Acknowledgements

This research work was sponsored by the Air Force Office of Scientific Research (AFOSR) under Grant F49620-01-1-0179. The authors acknowledge the support of Dr. Narendra S. Khot and Dr. Frank Eastep of Wright-Patterson Air Force Base, Ohio, for their valuable suggestions and as well as the support of Dr. John Edwards and Dr. David M. Schuster of NASA Langley Research Center, Hampton, Virginia, for providing the CAP-TSD code.

References

1. Johnson E., and Venkayya V.B.,(1988) "Automated Structural Optimization System (ASTROS)", *Volume-I Theoretical Manual*, U.S. Air Force Wright Aeronautical Labs. TR-88-3028.

2. Batina, J.T., Seidal, D.A., Bland, S.R. and Bennett, R.M.,(1990) "Unsteady Transonic Flow Calculations for Realistic Aircraft Configurations, *28th AIAA/ASME/ASCE/AHS Structures, Structural Dynamics and Materials Conference*, Monterey, CA, Paper No.: AIAA 1987-0850.

3. Jun, S., Tischler, V.A. and Venkayya, V.B.,(2002) "Multidisciplinary design optimization of a built-up wing structure with tip missile", *43rd AIAA/ASME/ASCE/AHS/ASC Structures, Structural Dynamics and Materials Conference*, Denver, Colorado, Paper No.: AIAA 2002-1421.

4. Guruswamy, G.P., Goorjian, P.M. and Tu, E.L., (1986) "Transonic Aeroelasticity of wings with Tip stores." AIAA paper 86-1007, pp 672-682.

5. Striz, A.G. and Jang, S.K., (1987) "Optimization of wing tip store modeling", *AIAA Journal of Aircraft*, 24(8), 516-517.

6. Raveh, D., Levy, Y., and Karpel, M., (2000) "Structural optimization using computational aerodynamics", *AIAA Journal*, 38(10), 1974-1982.

7. Kim, D. and Lee, I., (2001) "Transonic and supersonic flutter characteristics of a wing-box model with tip stores", *42nd AIAA/ASME/ASCE/AHS/ASC Structures, Structural Dynamics, and Material Conference and Exhibit*, Seattle, WA.

8. Rudisill, C.S., and Bhatia, K.G., (1971) "Optimization of complex structures to satisfy flutter requirements", *AIAA Journal*, 9(8), 1487-1491.

9. Khot, N., Zweber, J., and Eastep, F.,(2002) "Effect of frequency constraint optimization on the flutter characteristics of composite wings", *40th AIAA Aerospace Sciences Meeting & Exhibit*, Reno, Nevada, paper No.: AIAA 2002-0594.

10. Janardhan, S., Grandhi, R.V., Eastep, F., and Sanders, B.,(2003) "Design Studies of transonic flutter and limit-cycle oscillations of an aircraft wing/tip store", *44th AIAA/ASME/ASCE/AHS/ASC Structures, Structural Dynamics and Materials Conference*, Norfolk, Virginia, paper No.: AIAA 2003-1944.

Table I : Natural frequencies of initial and optimized designs (Cases III & IV)

S.No.	Initial Design (Hz)	Optimized design (case III constraints) (Hz)	Optimized design (case IV constraints) (Hz)
1	3.80565	4.6341	4.6386
2	7.84046	10.000	10.061
3	18.2321	19.345	20.139
4	20.3955	24.245	25.617
5	46.9985	46.537	47.923

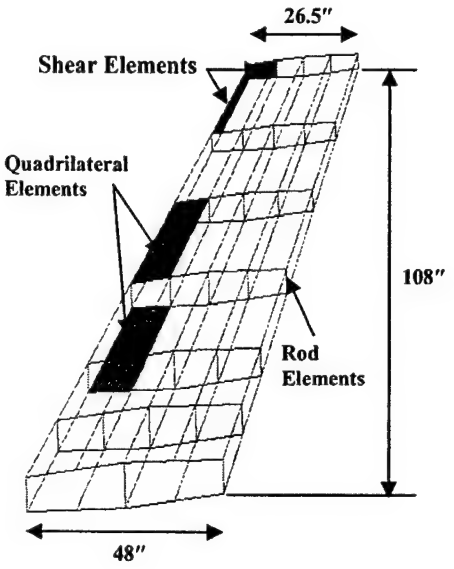

Figure 1: Wing structure finite element model

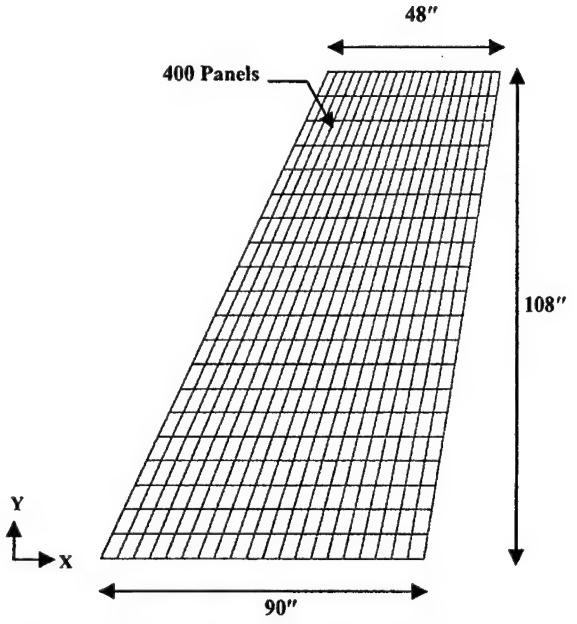

Figure 2: ASTROS aerodynamic model of wing

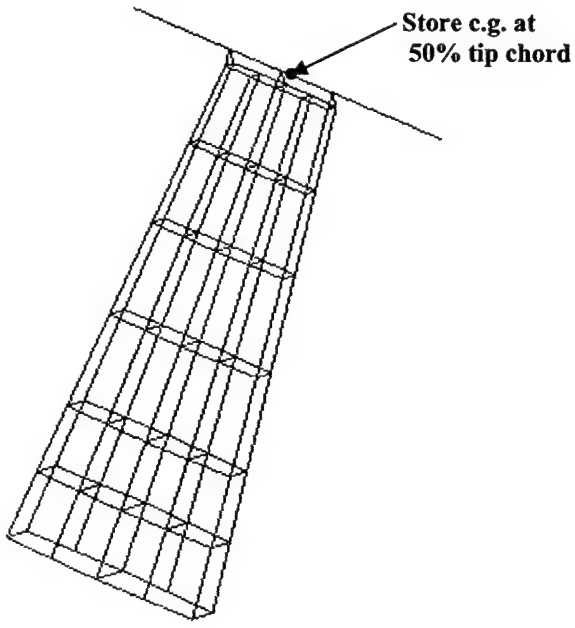

Figure 3: Finite element model of wing with tip store c.g. at 50% tip chord

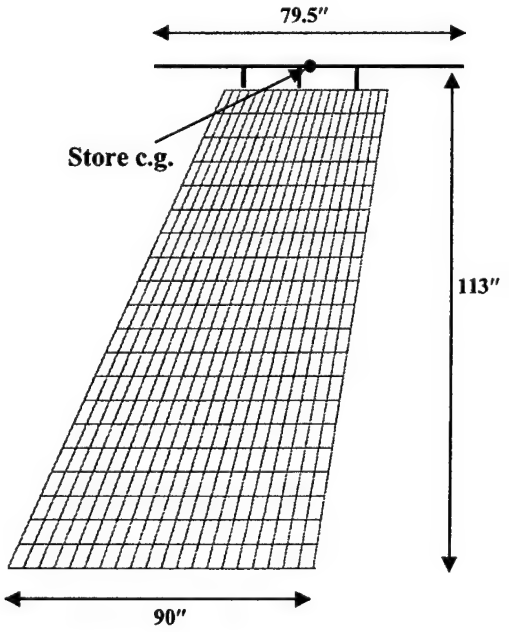

Figure 4: Aerodynamic model of wing with structural model of tip store c.g. at 50% tip chord

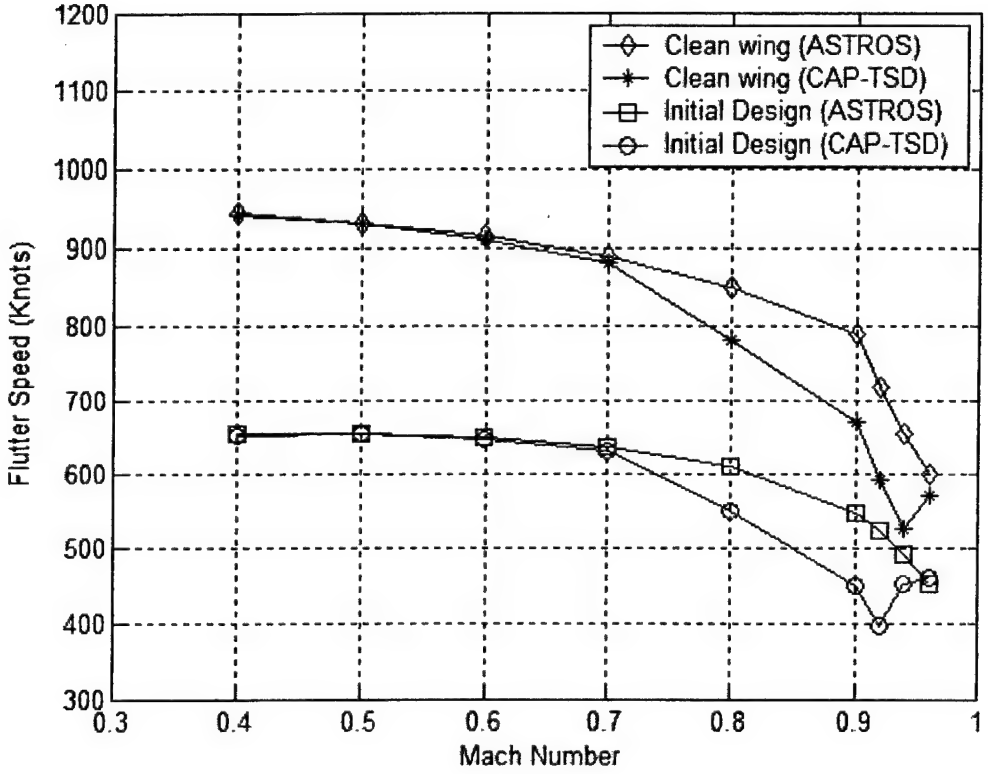

Figure 5: Comparison of flutter speeds of clean wing and initial wing/tip store designs using ASTROS and CAP-TSD for Mach numbers (0.4–0.96)

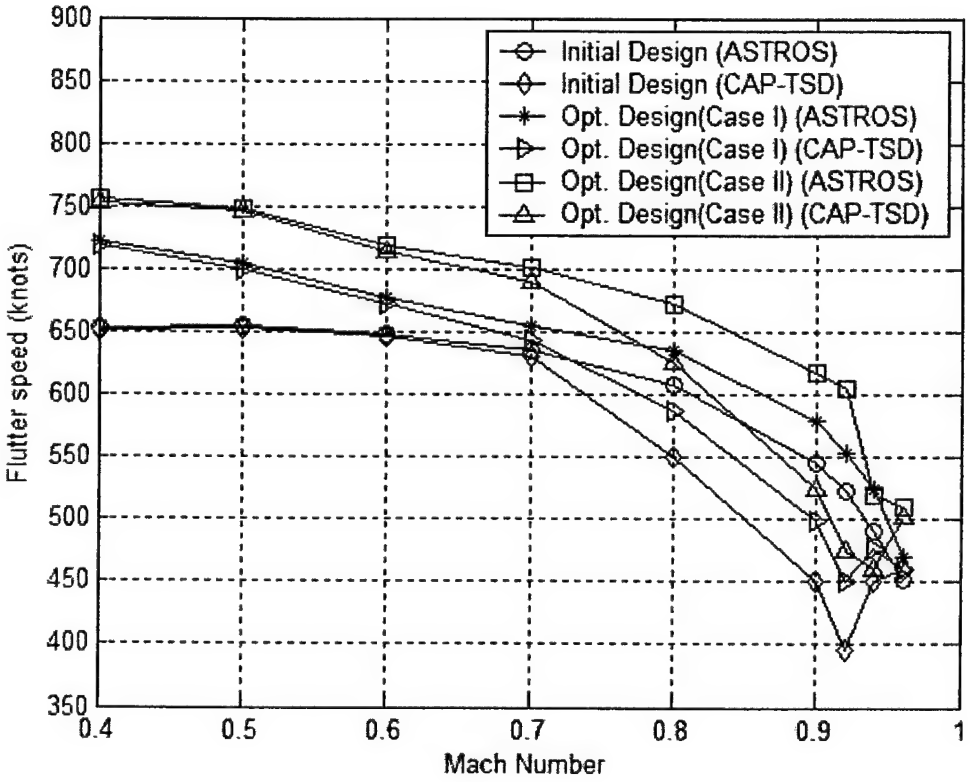

Figure 6: Comparison of flutter speeds of initial and optimized designs with Case I and Case II constraints using ASTROS and CAP-TSD for Mach number range (0.4–0.96)

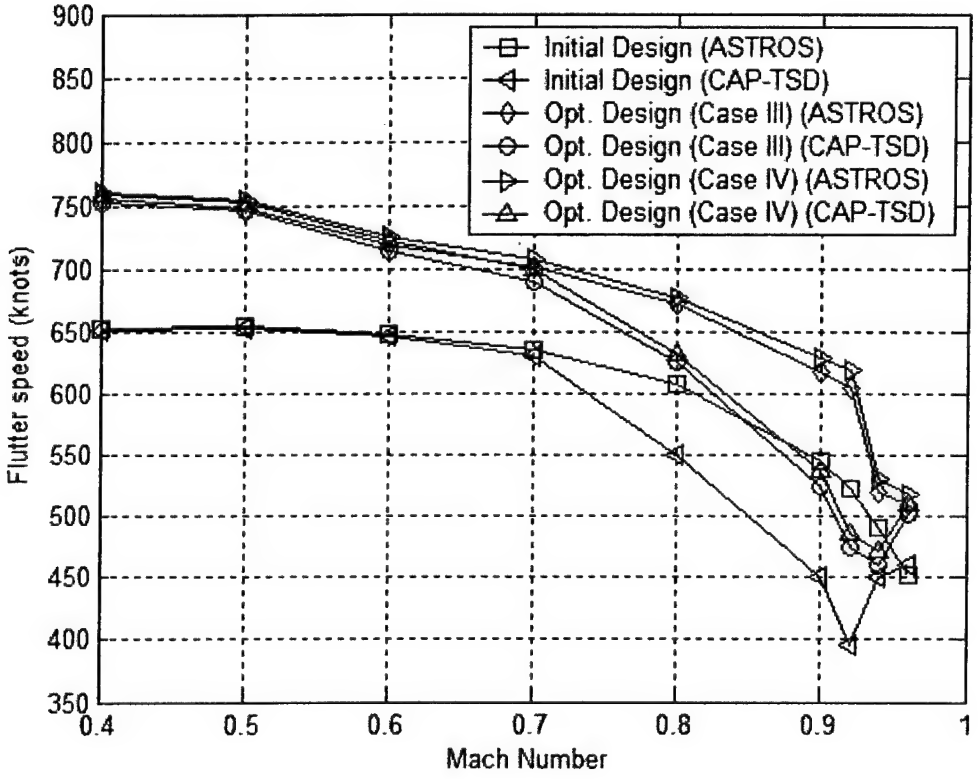

Figure 7: Comparison of flutter speeds of initial and optimized designs with Case III and Case IV constraints using ASTROS and CAP-TSD for Mach number range (0.4–0.96)

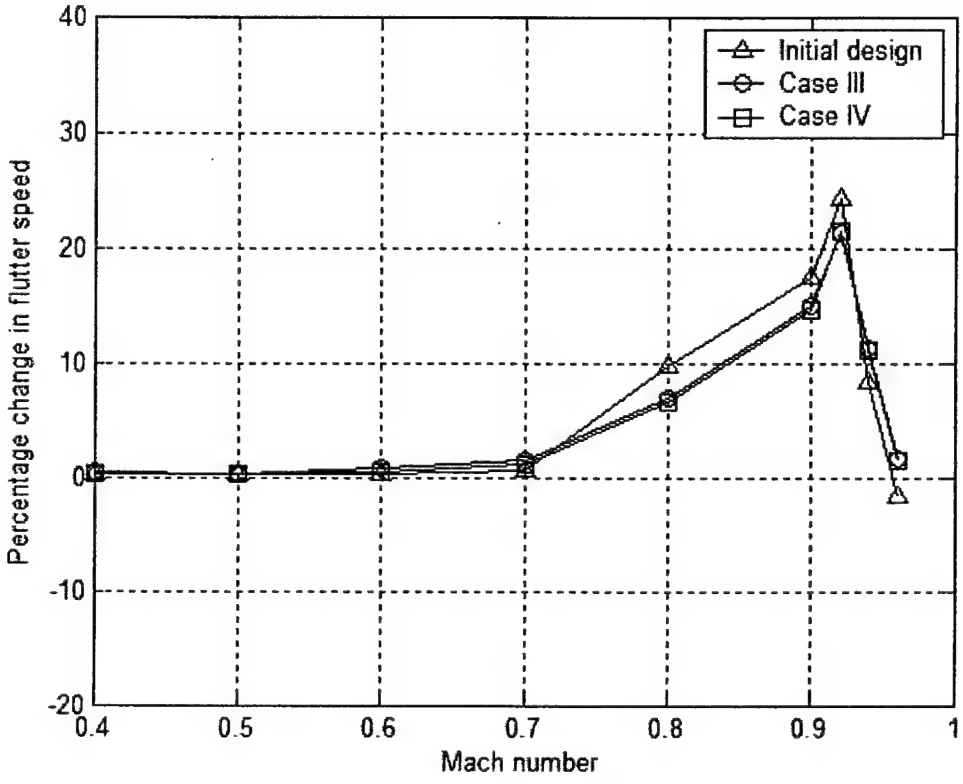

Figure 8: Comparison of percentage changes between ASTROS and CAP-TSD for various wing/store designs

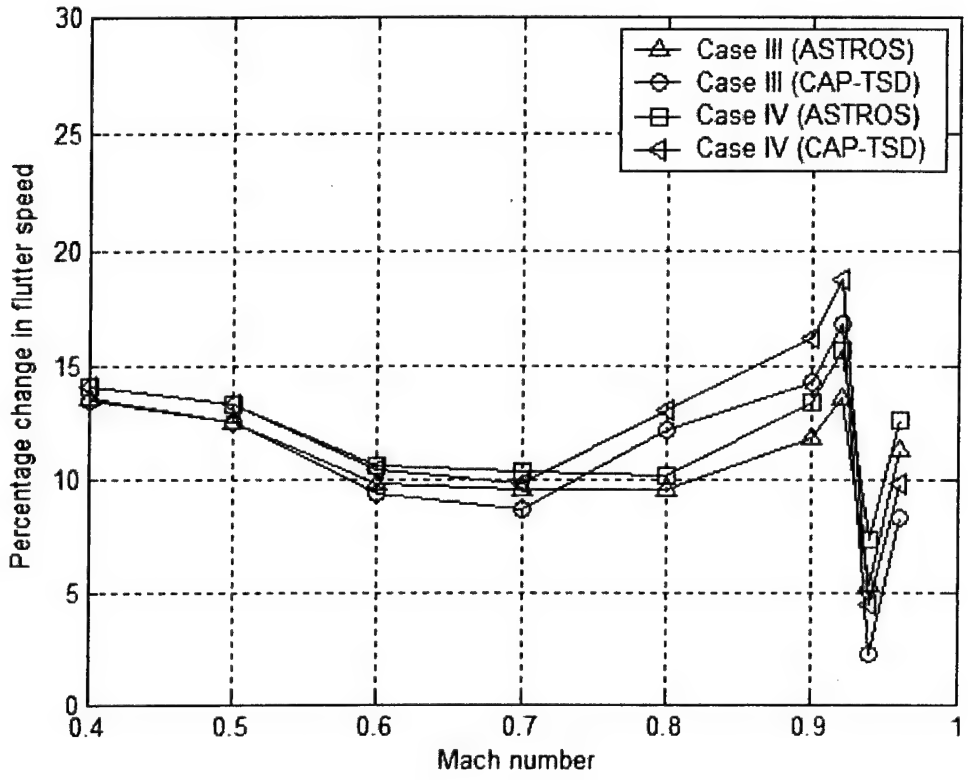

Figure 9: Comparison of percentage changes between Cases III and IV optimized designs using ASTROS and CAP-TSD for a Mach number range (0.4–0.96)

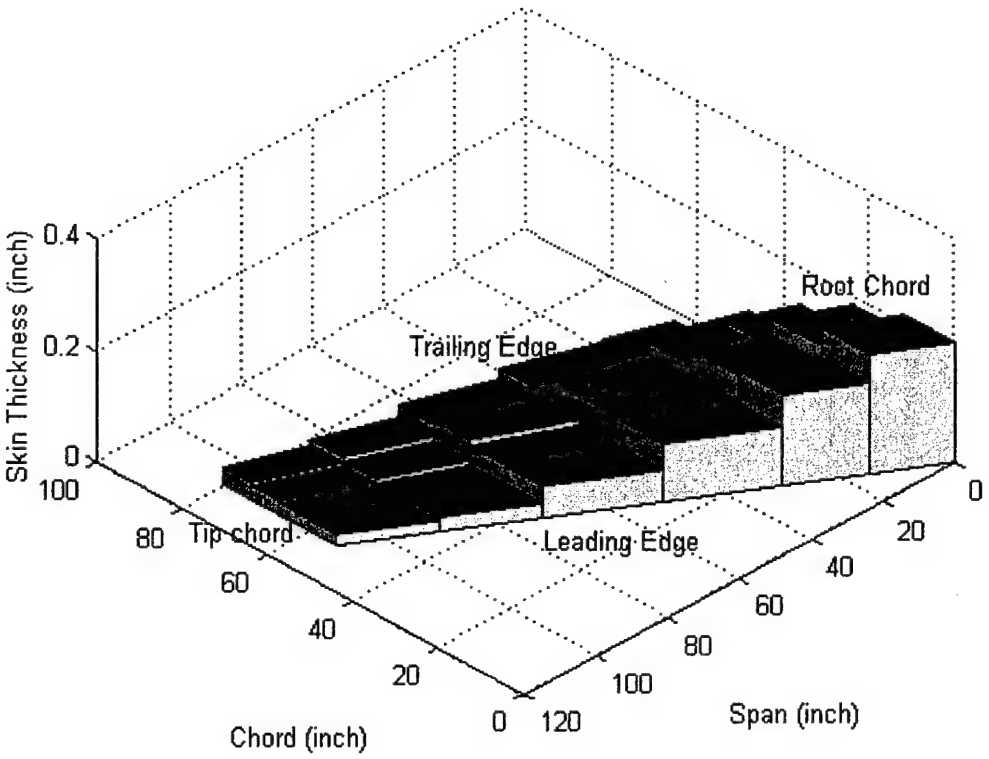

Figure 10: Upper skin thickness distribution of the initial wing design

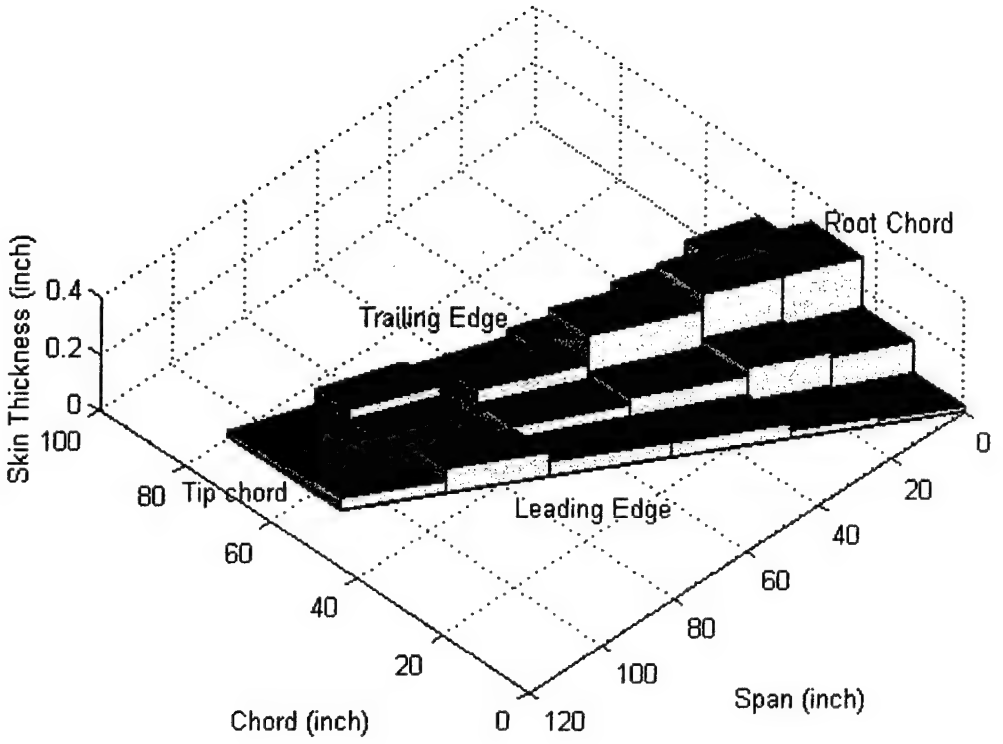

Figure 11: Upper skin thickness distribution of the optimized wing structure based on Case III constraints

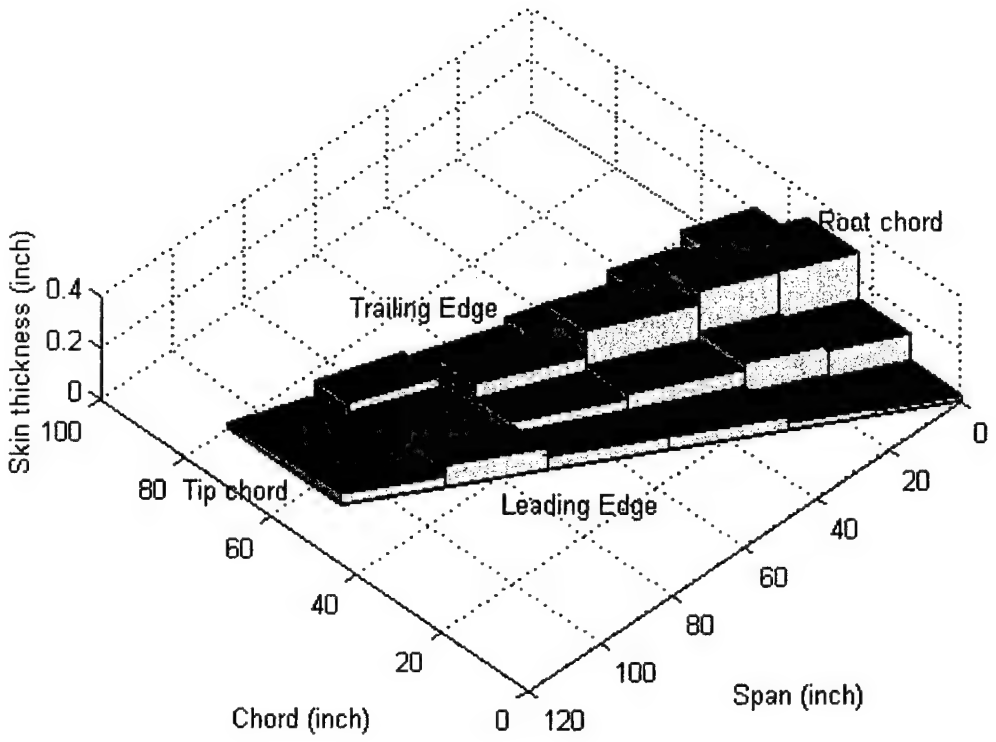

Figure 12: Upper skin thickness distribution of the optimized wing structure based on Case IV constraints

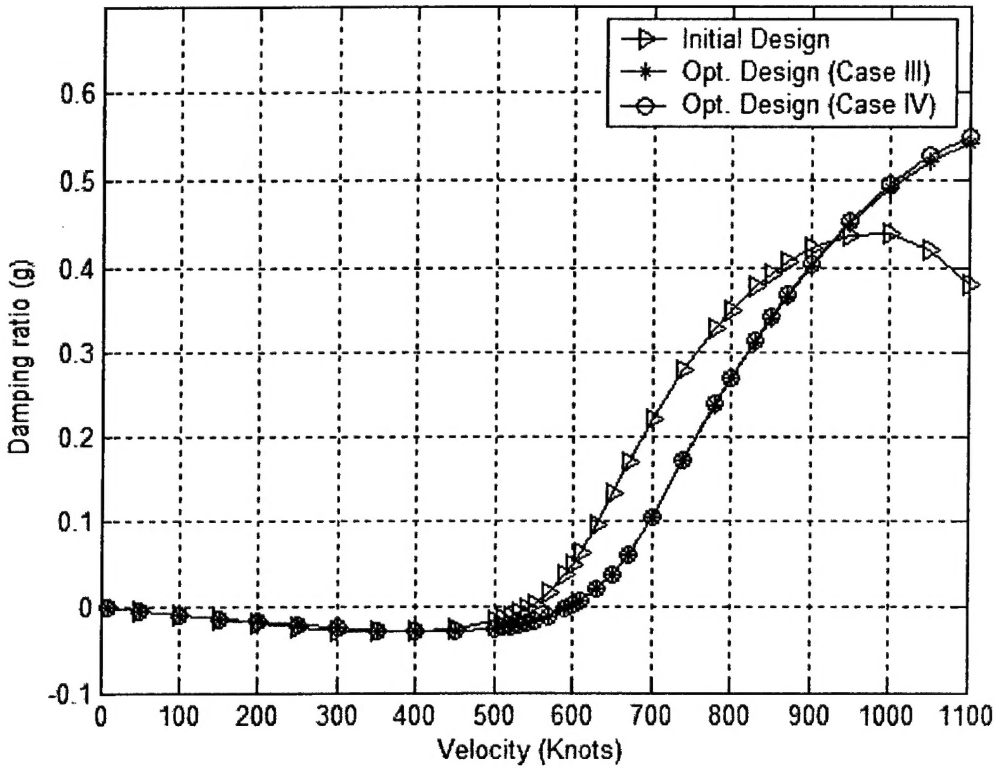

Figure 13: Comparison of flutter mode between initial and optimized wing designs based on Case III and IV constraints

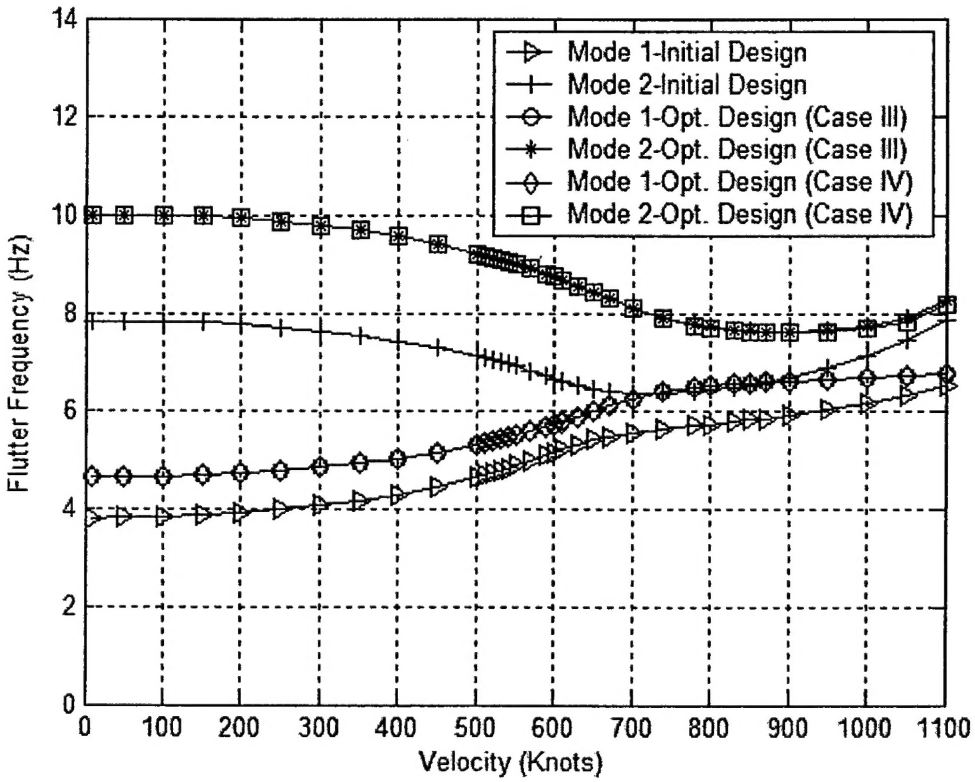

Figure 14: Velocity – frequency diagram representing comparison between initial and optimized wing designs (Cases III and IV) for flutter modes 1 and 2

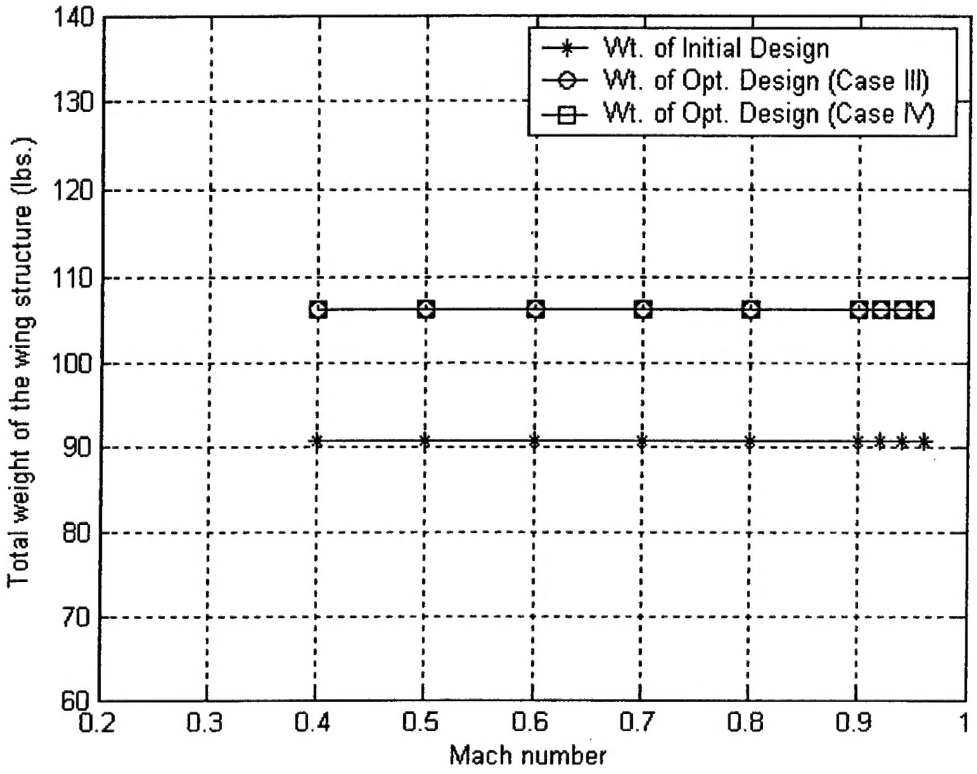

Figure 15: Comparison of structural weight for initial and optimized designs based on Case III and IV constraints

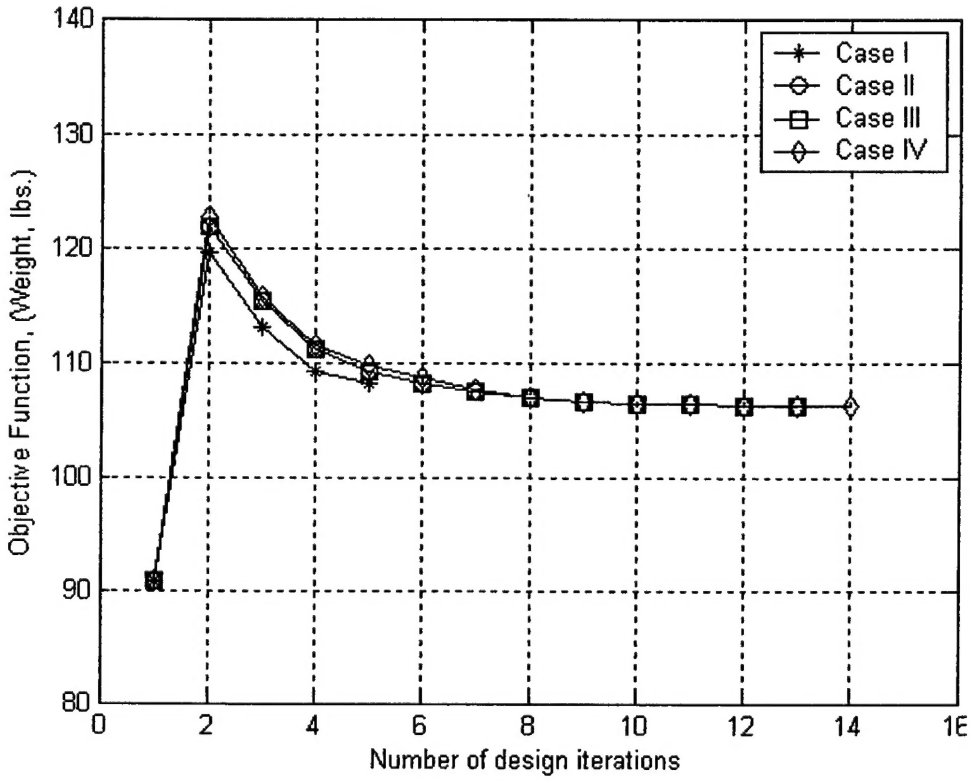

Figure 16: Design iteration histories for all optimization cases.